Int. J. Heat Mass Transfer. Vol. 32, No. 11, pp. 2047–2053, 1989
Printed in Great Britain

0017–9310/89 $3.00 + 0.00

Pseudosteady-state natural convection heat transfer inside spheres

J. HUTCHINS and E. MARSCHALL
Department of Mechanical and Environmental Engineering, University of California, Santa Barbara, CA 93106, U.S.A.

(*Received* 14 *September* 1988 *and in final form* 28 *February* 1989)

Abstract—A finite difference numerical method is used to study pseudosteady-state natural convection inside a closed spherical container. Stream functions, temperature contours, velocity profiles and Nusselt number relationships are presented. The results are compared with experimental data in the literature. It is found that the Nusselt number (for $Pr > 0.7$) correlates to the Rayleigh number by the following relation:

$$Nu = 1.19Ra^{0.2215}, \quad 10^5 < Ra < 10^8.$$

The pseudosteady-state analysis is extended to obtain the Nusselt number for a fluid having constant, uniformly distributed, internal heat sources. It is found that the Nusselt number (for $Pr > 0.7$) correlates to a modified Rayleigh number by the following relation:

$$Nu = 0.934(Ra^*)^{0.177}, \quad 7.2 \times 10^6 < Ra^* < 4.1 \times 10^{10}.$$

1. INTRODUCTION

NATURAL convection inside a spherical enclosure is a topic of interest and importance for heat transfer inside spherical fluid storage tanks and understanding heat and mass transfer inside spherical drops. A recently completed study [1] examines transient natural convection inside spherical containers and drops. A related area is the study of natural convection of enclosed, heat-generating fluids. For processes such as fermentation, liquid and gas radioactive waste heat removal and certain exothermic chemical reactions, the enclosed fluid may be modelled as having a constant, uniformly distributed heat source. Kee *et al.* [2] performed a preliminary investigation into the study of natural convection of a heat-generating fluid ($Pr = 0.7$) within closed vertical cylinders and spheres.

An alternative approach to studying heat-generating fluids is to employ the pseudosteady-state approach. In pseudosteady-state analysis, the temperature at the boundary is increased to maintain a constant temperature difference between the boundary and some place in the fluid. Thus, the driving force for heat transfer is kept constant. The results for the pseudosteady-state condition apply to the case of uniform heat generation at steady state. Note that the velocity field and temperature field for the pseudosteady-state condition will be inverted vertically compared to the fluid with uniform heat generation. Pseudosteady-state natural convection has been studied experimentally by Chow and Akins [3] for heat transfer inside spheres. Five different sized spheres were used to obtain a significant Rayleigh number variation. Lin and Akins [4, 5] numerically examined pseudosteady-state natural convection heat transfer inside vertical cylinders.

Chow and Akins [3] experimentally examined the pseudosteady-state natural convection of water inside five different sized spheres. Pseudosteady-state was maintained by steadily increasing the surrounding bath temperature outside the sphere so that the temperature difference between the outside bath and the center remained constant. Flow visualization was used to determine flow patterns within the spheres. Laminar flow was found to exist below Rayleigh numbers of about 8×10^7. The range of Rayleigh numbers examined was $8 \times 10^4 < Ra < 8 \times 10^7$. For reviewers of the work of Chow and Akins, it should be noted that they employ a radius based Rayleigh number whereas a diameter based Rayleigh number is employed in this paper.

In this work, pseudosteady-state was simulated using a finite difference technique to solve the vorticity, energy and stream function equations. The results of the simulation are compared with the experimental results of Chow and Akins. A correlation was found relating the Nusselt number to the Rayleigh number. For a heat-generating fluid, a modified Rayleigh number was defined on the basis of the volumetric heat generation rate. A correlation was found relating the Nusselt number to the modified Rayleigh number.

2. FORMULATION OF THE PROBLEM

This study considers a spherical enclosure containing a Newtonian fluid. It is assumed that:

(1) the fluid motion and temperature distribution are two-dimensional;

NOMENCLATURE

A	internal surface area of the spherical container [m^2]
A_0	volumetric internal heat source [W m^{-3}]
D	diameter of the spherical container [m]
g	gravitational acceleration [m s^{-2}]
Gr	Grashof number, $g\beta D^3(T_w-T_c)/\nu^2$
h	heat transfer coefficient, $Q/A(T_w-T_{ave})$ [W m^{-2} K^{-1}]
h_c	heat transfer coefficient, $Q/A(T_w-T_c)$ [W m^{-2} K^{-1}]
k	thermal conductivity [W m^{-1} K^{-1}]
Nu	Nusselt number, hD/k
Nu_c	Nusselt number, h_cD/k
Pr	Prandtl number, ν/α
Q	heat transfer rate [W]
r	radial coordinate [m]
R	dimensionless radial coordinate, r/R_0
R_0	radius of the spherical container [m]
Ra	Rayleigh number, $g\beta D^3(T_w-T_c)/k\nu$
Ra^*	modified Rayleigh number, $A_0g\beta D^5/k\nu\alpha$
t	time [s]
T	temperature [K]
T_{ave}	average temperature of fluid in the container [K]
T_b	initial temperature inside the container [K]
T_c	temperature at the center of the container [K]
T_w	temperature at $R=1$ [K]
T^*	dimensionless temperature, $(T-T_b)/(T_w-T_c)$
u	radial velocity [m s^{-1}]
U	dimensionless radial velocity, uR_0/α
v	tangential velocity [m s^{-1}]
V	dimensionless tangential velocity, vR_0/α.

Greek symbols

α	thermal diffusivity [m^2 s^{-1}]
β	coefficient of volumetric expansion [K^{-1}]
θ	angular coordinate
ν	kinematic viscosity [m^2 s^{-1}]
τ	dimensionless time, $\alpha\tau/R_0^2$
Ψ	dimensionless stream function
Ω	dimensionless vorticity.

(2) the fluid is viscous and incompressible;
(3) frictional heating is negligible;
(4) the fluid properties are constant except for the density variation with temperature;
(5) the density variation with temperature can be linearized over the range of interest (i.e. the Boussinesq approximation).

The flow field inside the container is conveniently described by the Navier–Stokes equations in spherical coordinates. Since the problem is two-dimensional due to the axisymmetry and the fact that the vorticity vector reduces to a scalar quantity, the stream function/vorticity formulation in spherical coordinates was employed [6]. Figure 1 shows the coordinate system and some nomenclature. The equations were put into non-dimensional form yielding the following:

vorticity equation

$$\frac{\partial\Omega}{\partial\tau}+U\left(\frac{\partial\Omega}{\partial R}-\frac{\Omega}{R}\right)+\frac{V}{R}\left(\frac{\partial\Omega}{\partial\theta}-\Omega\cot\theta\right)=Pr\left(\frac{\partial^2\Omega}{\partial R^2}+\frac{1}{R^2}\frac{\partial^2\Omega}{\partial\theta^2}+\frac{2}{R}\frac{\partial\Omega}{\partial R}+\frac{1}{R^2}\cot\theta\frac{\partial\Omega}{\partial\theta}-\frac{\Omega}{R^2\sin^2\theta}\right)-\frac{Gr\,Pr^2}{8}\left(\sin\theta\frac{\partial T^*}{\partial R}+\frac{\cos\theta}{R}\frac{\partial T^*}{\partial\theta}\right);\quad(1)$$

stream function equation

$$\Omega=\frac{1}{R\sin\theta}\left(\frac{\partial^2\Psi}{\partial R^2}+\frac{1}{R^2}\frac{\partial^2\Psi}{\partial\theta^2}-\frac{1}{R^2\tan\theta}\frac{\partial\Psi}{\partial\theta}\right);\quad(2)$$

velocities

$$U=-\frac{1}{R^2\sin\theta}\frac{\partial\Psi}{\partial\theta}\quad(3)$$

$$V=\frac{1}{R\sin\theta}\frac{\partial\Psi}{\partial R}.\quad(4)$$

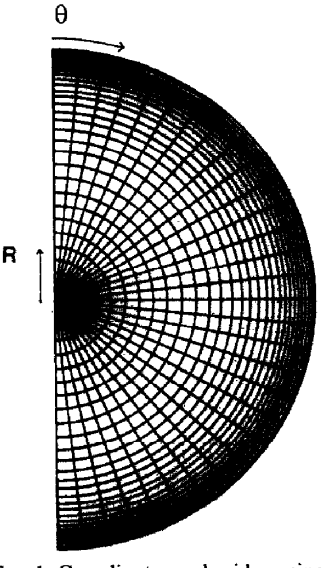

FIG. 1. Coordinates and grid spacing.

The temperature field of the container is described by the transient energy conservation equation in spherical coordinates

$$\frac{\partial T^*}{\partial \tau} + U\frac{\partial T^*}{\partial R} + \frac{V}{R}\frac{\partial T^*}{\partial \theta} = \frac{\partial^2 T^*}{\partial R^2} + \frac{2}{R}\frac{\partial T^*}{\partial R} + \frac{1}{R^2}\frac{\partial T^*}{\partial \theta^2} + \frac{\cot\theta}{R^2}\frac{\partial T^*}{\partial \theta}. \quad (5)$$

The boundary conditions are given as follows:

$$\Psi = 0 \quad \text{at } \theta = 0, \pi \quad (6)$$

$$\Omega = 0 \quad \text{at } \theta = 0, \pi \quad (7)$$

$$\partial T^*/\partial \theta = 0 \quad \text{at } \theta = 0, \pi \quad (8)$$

$$\Psi = 0 \quad \text{at } R = 1 \quad (9)$$

$$\Omega = \frac{1}{\sin\theta}\frac{\partial^2 \Psi}{\partial R^2} \quad \text{at } R = 1. \quad (10)$$

The boundary condition for T^* at $R = 1$ will be discussed later. The Nusselt number can be obtained from the gradient of the temperature at the boundary from the following relationship:

$$Nu = \frac{1}{T_w^* - T_{ave}} \int_0^\pi \left(\frac{\partial T^*}{\partial R}\right)_{R=1} \sin\theta \, d\theta. \quad (11)$$

The Nusselt number can also be obtained from the rate of enthalpy change of the fluid inside the spherical container. This results in the following relationship for the Nusselt number:

$$Nu = \frac{2}{3}\frac{1}{T_w^* - T_{ave}^*}\frac{dT_{ave}^*}{d\tau}. \quad (12)$$

The Nusselt numbers calculated from equations (11) and (12) should be identical. Both equations were employed to calculate the Nusselt number. The ratio of the two different Nusselt number calculations was used as a measure of health and accuracy of the numerical solution.

3. NUMERICAL METHOD

The vorticity transport, energy transport and stream function equations provide a complete description of the problem. The time-dependent vorticity transport and energy transport equations were solved employing the alternating direction implicit (ADI) finite difference technique. After each time step, a Gaussian successive over-relaxation technique was used to solve the stream function equation. The reader is directed to ref. [11] for a complete description of the solution technique. Salient features of the technique are discussed below.

The solution domain in the radial direction is divided into a grid with a variable radial step size. Fine radial spacing is employed near the boundary where the gradients are steep. Coarse spacing is used in the interior where the gradients are weak. The grid spacing employed used a radial step size of $\Delta R = 0.01$ at the interface. The radial step was increased by 10% at each radial node from the interface inward until a maximum radial increment of $\Delta R = 0.05$ was reached. This grid spacing is illustrated in Fig. 1. In the tangential direction, a step size of $\Delta\theta = 6°$ was used. The grid spacings radially and tangentially were found by decreasing the grid size by a factor of two and running the simulation. Repeatability of the Nusselt number was used as a measure of the adequacy of the grid spacing.

The discretization of the convective terms will now be discussed. A hybrid form of the central difference and the upwind difference technique similar to that discussed by Patankar [7] was employed. In Cartesian coordinates, the hybrid form uses the central difference technique if the cell Peclet number is $|Pe| < 2$ and the upwind difference technique if the cell Peclet number is $|Pe| > 2$. Thus, the accuracy of the central difference technique is obtained for small Peclet numbers where the diffusion term dominates the transport process. For large cell Peclet numbers, upwind differencing is employed where convection dominates the transport process. For large cell Peclet numbers, upwind differencing is employed where convection dominates the transport process. The technique works well for Cartesian coordinates and was modified for spherical coordinates. Details are given in ref. [1].

A quiescent, isothermal fluid ($T^* = 0$) was assumed as an initial condition. At $\tau = 0$, a step change of temperature ($T^* = 1$) was employed at the boundary ($R = 1$). A transient solution then progressed. At each time step the temperature at the center was monitored and the temperature at the boundary was increased to keep the dimensionless temperature difference between the wall and the center equal to one ($T_w^* - T_c^* = 1$). Determination of the pseudosteady-state condition was found by examining the Nusselt number. When the Nusselt number reached a constant unchanging value, the pseudosteady-state condition had been achieved.

The Rayleigh numbers modeled were 10^5, 10^6, 10^7 and 10^8 for Prandtl numbers of 0.7 and 8. It should be noted that Prandtl numbers greater than 8 were also simulated but the resulting Nusselt numbers were the same as for a Rayleigh number of 8. In addition, pseudosteady-state was modelled for $Ra = 5.2 \times 10^7$ with a Prandtl number of 4 as will be discussed below.

4. RESULTS

The following were reported by Chow and Akins:

(a) the tangential velocity profile along the horizontal of the sphere for $Ra = 5.2 \times 10^7$;

(b) the circulation center along the horizontal of the sphere as a function of Rayleigh number;

(c) the data to obtain their Nusselt number equation.

Each of these has been compared with the results generated by the simulation.

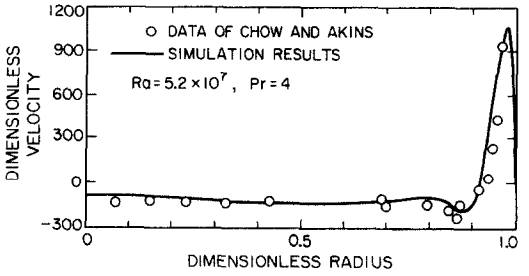

FIG. 2. Comparison of experimentally and numerically obtained velocities.

Table 1. Pseudosteady-state results

Ra	Pr	Nu	Nu_c
10^5	8	15.9	12.0
10^6	8	24.9	20.7
10^7	8	41.7	37.3
10^8	8	74.1	69.7
10^5	0.7	15.8	11.5
10^6	0.7	23.8	23.5
10^7	0.7	40.8	36.7
10^8	0.7	71.6	67.4
5.2×10^7	4	61.9	57.6

A tangential velocity profile along the horizontal of the sphere (i.e. $\theta = \pi/2$) for a Rayleigh number of 5.2×10^7 was reported. Since the Prandtl number was not reported, a Prandtl number of 4 was assumed (water at 43°C) for the simulation. This temperature is in the midrange of the temperatures studied by Chow and Akins and thus representative. The tangential velocity along the horizontal reported by Chow and Akins (converted into dimensionless velocity) and the simulation results are shown in Fig. 2. Positive velocities correspond to upward motion. The correlation is excellent.

The circulation center is the center of closed streamlines. Figure 5 will be discussed later but the reader should examine the left-hand side of Fig. 5 in order to understand circulation in the container. The left-hand side of the figure shows the closed streamlines. The maximum downward velocity predicted by the simulation occurred inside the circulation center. This same phenomenon is reported by Chow and Akins and is seen in the experimental data shown in Fig. 2. Chow and Akins suggest that this phenomenon may be due to the higher temperature and thus the lower viscosity near the wall. However, the temperature differences they used were of the order of 2.5°C. Such a small temperature variation probably would not have caused a significant viscosity variation. Also, the simulation predicts a similar downward velocity peak and the viscosity in the simulation is constant. At present, an explanation of this phenomenon is lacking but the phenomenon is seen in both the experimental data and the simulation results.

The location of the circulation center along the horizontal as a function of Rayleigh number will now be discussed. The circulation center as a function of Rayleigh number as obtained from the simulation and as reported by Chow and Akins is shown in Fig. 3. The correlation between the experimental data and the simulation results is good. Figure 3 shows that the circulation moves towards the wall for increasing Rayleigh numbers.

The Nusselt number relationships obtained by Chow and Akins and from the simulation results will now be discussed. The Nusselt numbers obtained from the simulation are shown in Table 1. Two Nusselt numbers are reported: Nu is based upon the common definition of the driving force of $T_w - T_{ave}$; Nu_c is based upon Chow and Akins' definition of the driving force of $T_w - T_c$. Examination of Table 1 shows that the Nusselt numbers (Nu and Nu_c) are relatively independent of Prandtl number in the range of $0.7 < Pr < 8$. Other simulation runs were carried out at higher Prandtl numbers and no dependence on Prandtl number was found. A least squares fit of the data in Table 1 yields

$$Nu = 1.19 Ra^{0.2215} \tag{13}$$

$$Nu_c = 0.655 Ra^{0.2521}. \tag{14}$$

Chow and Akins reported that a least squares fit of their experimental data yielded the following equation:

$$Nu_c = 0.54 Ra^{0.3}. \tag{15}$$

Figure 4 shows the data of Chow and Akins, their Nusselt number relationship (equation (15)) and the

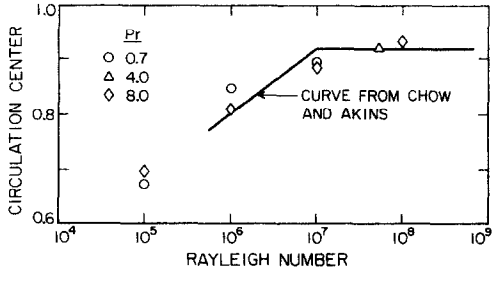

FIG. 3. Dependence of location of circulation center on Rayleigh number.

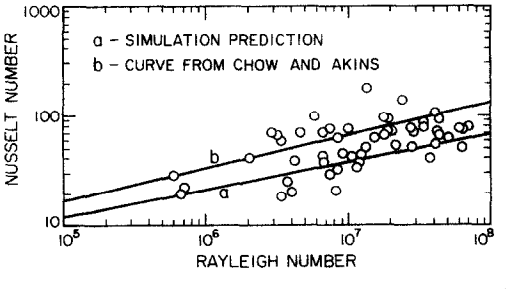

FIG. 4. Comparison of experimentally and numerically obtained Nusselt numbers.

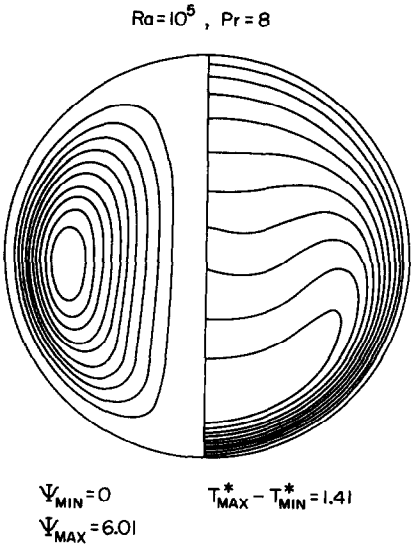

FIG. 5. Streamline and isotherm plot.

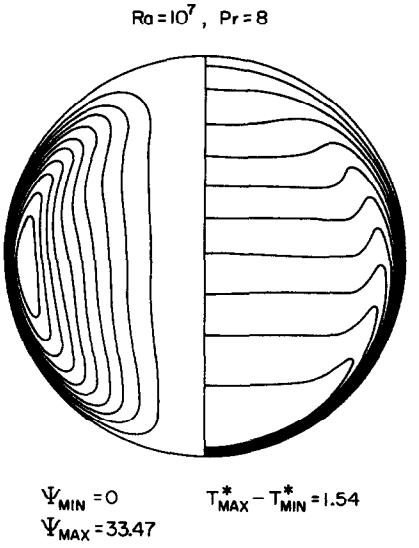

FIG. 7. Streamline and isotherm plot.

Nusselt number relationship obtained from the present study (equation (14)). As can be seen, the curve obtained from the simulation results is lower but nearly parallel to the experimentally derived curve. The fact that the two curves are nearly parallel indicates that the simulation and the data track one another quite well. The reason that the experimental curve may be higher than the simulation curve is due to the assumptions made to obtain the experimental Nusselt number data. In their work, Chow and Akins estimated the average inside wall temperature. They knew and controlled the surrounding bath temperature. The average inside wall temperature was calculated through knowledge of the wall thickness, its conductivity, the average heat flux and the bath temperature. Without explanation, Chow and Akins state in their paper that the resistance to heat transfer of the inside film, the wall and the outside film were estimated at 70, 25 and 5%, respectively. If these resistances are incorrect, the calculated inside wall temperature used by Chow and Akins for their Rayleigh and Nusselt numbers would have been in error. In addition, the wall temperature may not have been constant as a function of angle (θ) due to the influence of heat transfer through the container and the surrounding water bath.

It is felt that the more important correlation of the simulation curve and the experimental curve is that the slopes are similar and track one another well.

The results of the simulation were used to obtain a clearer understanding of pseudosteady-state natural convection. Figures 5–8 are streamline and isotherm

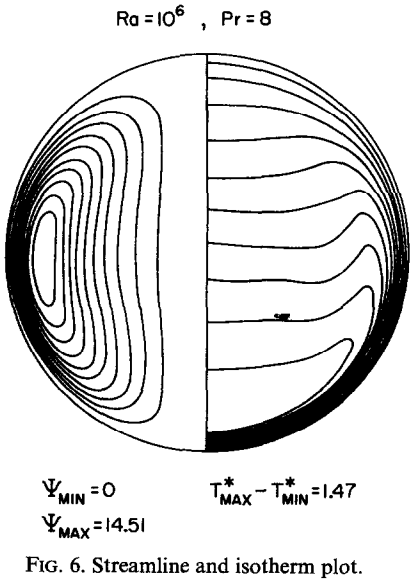

FIG. 6. Streamline and isotherm plot.

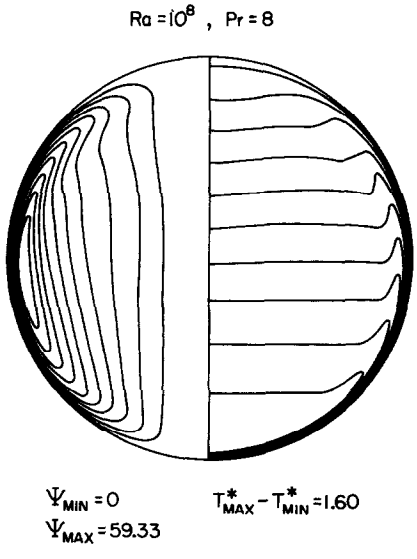

FIG. 8. Streamline and isotherm plot.

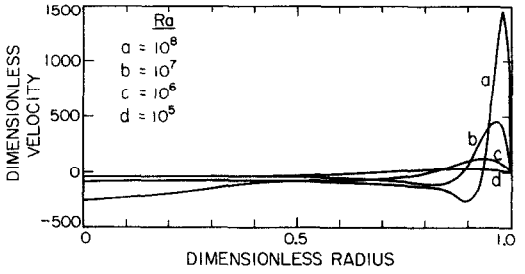

FIG. 9. Tangential velocity vs horizontal radius.

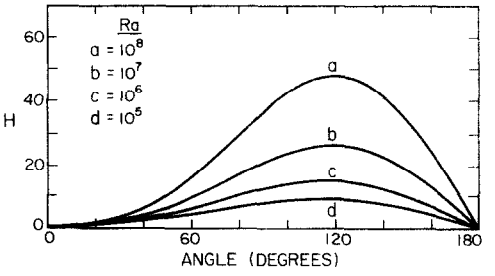

FIG. 11. Values of H vs angle.

plots of a fluid ($Pr = 8$) at Rayleigh numbers of 10^5, 10^6, 10^7 and 10^8, respectively. Equally spaced streamlines are shown on the left-hand side of the figures. The minimum and maximum streamline values are noted below the plots. The maximum streamline value corresponds to the center of circulation. The dimensionless temperature difference between the maximum and minimum temperature is noted below the isotherm plots.

Examination of the streamline plots indicates a circulation pattern around the circulation center. Fluid flows up the wall and down through the center. The circulation center moves closer to the wall as the Rayleigh number increases. Figure 9 displays the dimensionless tangential velocity along the horizontal as a function of Rayleigh number. The maximum tangential velocity increases dramatically with Rayleigh number.

Examination of the isotherm plots indicates that high temperature gradients exist near the wall in the lower hemisphere. The magnitude of the gradients increases as the Rayleigh number increases. The minimum temperature in the container occurs near the bottom of the container.

Figure 10 displays the dimensionless temperature gradient at the wall vs angular position. The gradient is small near the top of the container ($\theta = 0°$) and increases as the angular position increases. The maximum gradient occurs at the bottom of the container ($\theta = 180°$) for all Rayleigh numbers displayed.

Figure 11 displays the value H which is proportional to the local heat flow at the wall as a function of angular position. The value H is defined as

$$H = \frac{\dfrac{\partial T^*}{\partial R}\sin\theta}{T^*_w - T^*_{ave}}. \tag{16}$$

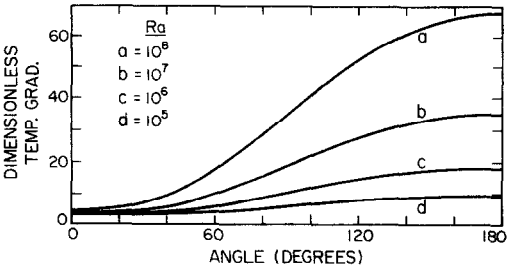

FIG. 10. Temperature gradient at wall vs angle.

It can be shown that the Nusselt number is

$$Nu = \int_0^{\pi} H \, d\theta. \tag{17}$$

The maximum value of H is the location of maximum heat transfer and occurs at an angular position of 110-120° in Fig. 11 for all displayed Rayleigh numbers.

The relationship of pseudosteady-state natural convection to that for heat generating fluid will now be discussed. The Nusselt numbers are identical for the two processes for the same Rayleigh number. However, the salient parameter which characterizes a heat generating fluid is the volumetric internal heat generation rate (A_0). A modified Rayleigh number (Ra^*) is defined for a heat generating fluid by

$$Ra^* = \frac{A_0 g\beta D^5}{k\nu\alpha}. \tag{18}$$

A simple energy balance on the container yields

$$A_0 = \frac{6h(T_w - T_{ave})}{D}. \tag{19}$$

Substituting equation (19) into equation (18) gives

$$Ra^* = \frac{6h(T_w - T_{ave})g\beta D^4}{k\nu\alpha}. \tag{20}$$

However, recognizing that the heat flow at the wall can be defined by

$$Q = hA(T_w - T_{ave}) \tag{21}$$

or

$$Q = h_c A(T_w - T_c) \tag{22}$$

it follows that

$$T_w - T_{ave} = \frac{h_c}{h}(T_w - T_c). \tag{23}$$

Substituting equation (23) and the definition of Ra into equation (20) gives

$$Ra^* = 6Nu\left(\frac{Nu_c}{Nu}\right)Ra. \tag{24}$$

Substituting equations (14) and (15) into equation (24) and performing the necessary algebra yields the following relationship for the Nusselt number as a function of the modified Rayleigh number:

$$Nu = 0.934(Ra^*)^{0.177},$$

$$7.2 \times 10^6 < Ra^* < 4.1 \times 10^{10}. \quad (25)$$

Thus, for a fluid with a known heat generation rate, equation (25) allows the prediction of the Nusselt number from which the steady mean fluid temperature can be determined.

REFERENCES

1. J. Hutchins, Transient natural convection inside rigid drops in a liquid–liquid direct-contact heat exchanger, Ph.D. dissertation, University of California, Santa Barbara, California (June 1988).
2. R. Kee, C. Landrum and J. Miles, Natural convection of a heat generating fluid within closed spheres and cylinders, *ASME J. Heat Transfer* **98**, 55–61 (1976).
3. M. Chow and R. Akins, Pseudosteady-state natural convection inside spheres, *ASME J. Heat Transfer* **97**, 54–59 (1975).
4. Y. Lin and R. Akins, Pseudo-steady-state natural convection heat transfer inside a vertical cylinder, *ASME J. Heat Transfer* **108**, 310–316 (1986).
5. Y. Lin and R. Akins, Thermal description of pseudo-steady-state natural convection inside a vertical cylinder, *Int. J. Heat Mass Transfer* **29**, 301–307 (1986).
6. P. Roache, *Computational Fluid Dynamics*. Hermosa, Albuquerque (1972).
7. S. Patankar, *Numerical Heat Transfer and Fluid Flow*. Hemisphere, Washington, DC (1980).

TRANSFERT DE CHALEUR PAR CONVECTION NATURELLE PSEUDO-STATIQUE DANS DES SPHERES

Résumé—Une méthode numérique aux différences finies est utilisée pour étudier la convection naturelle pseudo-statique dans un récipient sphérique fermé. On présente les fonctions de courant, les champs de température, les profils de vitesse et les formules du nombre de Nusselt. Les résultats sont comparés avec les données expérimentales disponibles. On trouve que le nombre de Nusselt (pour $Pr > 0{,}7$) est lié au nombre de Rayleigh par la relation:

$$Nu = 1{,}19Ra^{0{,}2215}, \quad 10^5 < Ra < 10^8.$$

L'analyse pseudo-statique est élargie pour obtenir le nombre de Nusselt pour un fluide ayant des sources de chaleur internes constantes et uniformément distribuées. On trouve que le nombre de Nusselt (pour $Pr > 0{,}7$) est donné par:

$$Nu = 0{,}934(Ra^*)^{0{,}177}, \quad 7{,}2 \times 10^6 < Ra^* < 4{,}1 \times 10^{10}.$$

WÄRMEÜBERGANG BEI PSEUDOSTATIONÄRER FREIER KONVEKTION IN EINEM KUGELBEHÄLTER

Zusammenfassung—Pseudostationäre freie Konvektion in einem Kugelbelhälter wurde mit Hilfe eines Differenzenverfahrens analysiert. Als Ergebnisse wurden Angaben über Stromfunktionen, Isothermen, Geschwindigkeitsprofile und Korrelationen für die Nusselt-Zahlen erhalten. Die berechneten Ergebnisse wurden mit experimentellen Daten aus der Literatur verglichen. Der folgende Zusammenhang zwischen der Nusselt-Zahl und der Rayleigh-Zahl wurde gefunden:

$$Nu = 1{,}19Ra^{0{,}2215}, \quad 10^5 < Ra < 10^8, \quad Pr > 0{,}7.$$

Die Analyse wurde den Fall ausgedehnt, in dem in dem Behälter gleichförmig verteilte wärmequellen existieren. Für diesen Fall wurde folgende Beziehung gefunden:

$$Nu = 0{,}934(Ra^*)^{0{,}177}, \quad 7{,}2 \times 10^6 < Ra^* < 4{,}1 \times 10^{10}, \quad Pr > 0{,}7.$$

ПСЕВДОСТАЦИОНАРНЫЙ ЕСТЕСТВЕННОКОНВЕКТИВНЫЙ ТЕПЛОПЕРЕНОС ВНУТРИ СФЕРЫ

Аннотация—Численным методом конечных разностей исследуется псевдостационарная естественная конвекция внутри замкнутого сферического контейнера. Представлены зависимости для функций тока, профилей температуры и скорости чисел Нуссельта. Результаты сравниваются с имеющимися в литературе экспериментальными данными. Найдена следующая зависимость между числами Нуссельта (при $Pr > 0{,}7$) и Рэлея:

$$Nu = 1{,}19Ra^{0{,}2215}, \quad 10^5 < Ra < 10^8.$$

Обобщен анализ псевдостационарного процесса с целью определения числа Нуссельта в случае жидкости с постоянными равномерно распределенными внутренними источниками тепла. Обнаружено, что число Нуссельта (при $Pr > 0{,}7$) определяется следующим образом через модифицированное число Рэлея:

$$Nu = 0{,}934(Ra^*)^{0{,}177}, \quad 7{,}2 \times 10^6 < Ra^* < 4{,}1 \times 10^{10}.$$